Chemical Engineering Journal 245 (2014) 166–172

Contents lists available at ScienceDirect

Chemical Engineering Journal

journal homepage: www.elsevier.com/locate/cej

Synthesis of starch-derived mesoporous carbon for electric double layer capacitor

Mingbo Wu [a,*], Peipei Ai [a], Minghui Tan [a], Bo Jiang [a], Yanpeng Li [a], Jingtang Zheng [a,*], Wenting Wu [a], Zhongtao Li [a], Qinhui Zhang [a,*], Xiaojun He [b,*]

[a] State Key Laboratory of Heavy Oil Processing, China University of Petroleum, Qingdao 266580, China
[b] School of Chemistry and Chemical Engineering, Anhui University of Technology, Ma'anshan 243002, China

HIGHLIGHTS

- Mesoporous carbon (MC) was prepared from starch by simultaneous template method.
- Starch-derived MC has high capacitance retention and rate capability.
- Starch-derived MC with high mesoporosity is a competitive material for capacitor.

GRAPHICAL ABSTRACT

Starch-derived mesoporous carbon with well-developed mesoporosity and superior electrochemical performance was prepared by simply simultaneous template method.

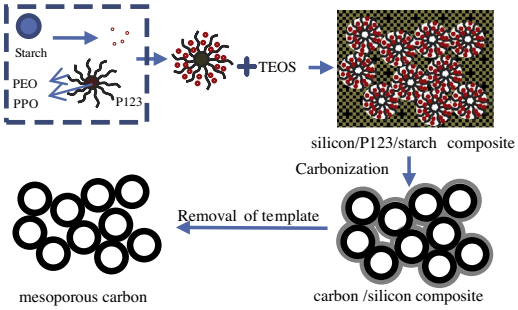

ARTICLE INFO

Article history:
Received 10 September 2013
Received in revised form 2 January 2014
Accepted 6 February 2014
Available online 15 February 2014

Keywords:
Starch
Mesoporous carbon
Simultaneous template method
Crystallization time
Electric double layer capacitor

ABSTRACT

Starch-derived mesoporous carbons (SMCs) with well-developed mesoporosity were prepared by simultaneous template method, wherein the template and the carbon precursor were simultaneously synthesized. The synthesis mechanism and the effect of crystallization time on the pore structure of the resultant SMCs were investigated by N_2 adsorption, FTIR, Raman and TEM. The electrochemical properties of SMC electrodes were studied by constant current charge–discharge, cyclic voltammetry and electrochemical impedance spectroscopy. The results showed that the BET surface area, total pore volume and mesoporosity of prepared SMCs went through maximum as the crystallization time increased. At 24 h of the crystallization time, the BET surface area of obtained SMC (named SMCT-24) was as high as 1157 $m^2\ g^{-1}$, and its total pore volume reached 0.97 $cm^3\ g^{-1}$, 95.0% of which belonged to mesopore. The specific capacitance of SMCT-24 capacitor was as high as 144 $F\ g^{-1}$ at the current density of 0.05 $A\ g^{-1}$ in 6 M KOH electrolyte, and remained at 127 $F\ g^{-1}$ after 1000 cycles, indicating that SMC could be a promising electrode material for electric double layer capacitor with high electrochemical performance.

1. Introduction

Electric double layer capacitor (EDLC) has drawn considerable attention and been regarded as an efficient energy-storage device

* Corresponding authors. Tel.: +86 532 8698 3452/3451/1855/555 2311 807.
E-mail addresses: wumb@upc.edu.cn (M. Wu), jtzheng03@163.com (J. Zheng), qhzhang@upc.edu.cn (Q. Zhang), xjhe@ahut.edu.cn (X. He).

http://dx.doi.org/10.1016/j.cej.2014.02.023
1385-8947/

for its high power density, long cycle life and low maintenance cost [1]. Based on the electrochemical charge accommodation at the electric double layer and the occurrence of Faradic reactions [2–6], the electrochemical performance of EDLC largely depends on the electrode materials. Among the electrode materials, porous carbons including mesoporous carbons (MCs) and microporous carbons have been paid much attention due to their unique physicochemical properties, high specific surface area and low cost [7–13]. The large surface area of porous carbons usually has been considered as a basic guiding principle for larger capacity [14,15]. However, only the pores that electrolyte ions can access contribute to the double layer capacitance. Therefore, the pore size distribution of porous carbons plays important role in their electrochemical performances.

Template method is one of the most efficient methods to prepare MCs with high specific surface area and uniform mesopores [16–23]. However, it is rather difficult to accurately control the pore structure of MCs as a result of the unchangeable template fabric. In order to control the textures of both the template and the carbon precursor, a simply simultaneous template method was forwarded in this experiment and achieved by regulating the sol–gel reaction conditions, wherein the template material and the carbon precursor were simultaneously synthesized. This process makes it possible to obtain MCs with tunable pore structure.

As a kind of natural polysaccharide compound, starch is plentiful and contains more than 49% of oxygen. High content of oxygen in starch results in the surface of starch-derived porous carbons with lots of hydrophilic groups, which can be easily regulated toward different applications. Additionally, starch-derived porous carbons are inexpensive and environmental friendly. To our knowledge, the effect of pore size distribution of SMC on its electrochemical performance has not been systematically investigated. Herein, SMC with superior capacitive behavior and better power output performance was synthesized by a simultaneous template method. The pore size distribution and electrochemical performance of SMC were characterized, and the internal relationship between them was discussed.

2. Experimental

2.1. Preparation and characterization of SMC

All chemical reagents and raw materials used were provided by Sinopharm Chemical Reagent Company, China. 4.0 g starch, 8.0 g $EO_{20}PO_{70}EO_{20}$ copolymer (Pluronic P123) and HCl solution (320 mL, 2 M) were added to a reaction vessel. The mixture was stirred at 35 °C in a water bath for 6 h until P123 was completely dissolved. Tetraethoxysilane (TEOS, 18.4 mL) as silica source was added to the as-prepared solution. After stirred for 24 h, the solution was then placed in a closed teflon vessel and kept for 12, 24 or 48 h at 100 °C without stirring (corresponding to SMCT-12, SMCT-24, SMCT-48 of final SMC samples, respectively). The precipitate was washed by distilled water and dried at 35 °C in vacuum oven. The obtained precipitate (1 g) was then mixed with 10 mL deionized water and 98 wt% H_2SO_4 (1 mL), stirred for 12 h, and pre-carbonized at 100 °C for 6 h. The pre-carbonized sample was volatilized and the solid residue was heated at 1 °C min^{-1} and carbonized at 850 °C for 2 h in nitrogen. The resultant carbon/silica composite was washed with 40 wt% HF solution to extract silica from the carbon framework. Finally, SMC was obtained by thoroughly washing with deionized water and subsequent drying.

The chemical functional groups of as-made SMCs were characterized by Fourier transform infrared spectrometry (FTIR) (Thermo Nicolet NEXUS 670, USA). The BET surface area and the pore size distribution of SMCs were analyzed by nitrogen adsorption (Micromeritics ASAP 2020 sorption analyzer, USA). The surface morphology of SMCs was characterized by transmission electron microscopy (TEM) (JEM-2100UHR, Japan). The crystallinity of SMCs were labeled by Raman analysis (Renishaw inVia 2000 Raman Microscope, Renishaw Plc., U.K.).

2.2. Electrochemical measurement

In order to characterize the electrochemical performance of prepared SMCs, SMC powder, acetylene black, and polytetrafluoroethylene (PTFE) were thoroughly mixed at weight ratios of 85:5:10 in ethanol until slurry formed. The electrodes were prepared by pressing the above slurry on the foam nickel with diameter of 12 mm at 20 MPa for 30 s, and dried in vacuum at 100 °C for 1 h. Finally, button-type capacitor was assembled with two SMC electrodes separated by a polypropylene membrane, and 6 M KOH solution as electrolyte.

Galvanostatic charge/discharge analysis was studied on a land cell tester (Land, CT-2001A, China). Cyclic voltammetry (CV) and electrochemical impedance spectroscopy (EIS) tests were carried out on an electrochemical workstation (PARSTAT 4000, Princeton, USA). The potential range of CV was −0.5–0.5 V, and the Nyquist plot was recorded at the frequency from 100 kHz to 0.01 Hz. All electrochemical measurements were carried out at room temperature.

3. Results and discussion

3.1. Synthesis mechanism

Fig. 1 presents the synthesis schematic of SMC, wherein the template and the carbon precursor are simultaneously synthesized. At the initial stage of synthesis, starch is hydrolyzed under the catalysis of hydrochloric acid. As a kind of good amphiphilic block copolymer, P123 can self-assemble into spherical micelles with a hydrodynamic radius of 10 nm due to its mesostructural ordering properties and amphiphilic character [24,25]. Most starch hydrolyzates with hydroxyl groups locate at the interfaces of hydrophilic groups (PEO) of P123 molecules, and form a hybrid carbon precursor via hydrogen bond. When TEOS as the silica precursor is added into the above mixture, its hydrolyzates can produce small size oligomers with Si–OH, which also can connect with PEO of P123 through hydrogen bond, thus forming silicon/P123/starch co-assembly system. With the increasing crystallization time, the silicon/P123/starch system develops, and a solid composite can be obtained. P123 and starch in silicon/P123/starch composite can further crosslink with the help of sulphuric acid. After carbonization, they were turned into the carbon/silicon composite. Finally, SMC was obtained after silicon being removed by hydrofluoric acid.

3.2. Porosity characterization

Fig. 2 shows the typical hysteresis loops with capillary condensation ($P/P_0 > 0.45$) of SMCT-12, SMCT-24 and SMCT-48. All hysteresis loops correspond to type-IV according to the IUPAC classification, basically demonstrating their mesoporous structures. Moreover, the hysteresis loops of SMCs in Fig. 2 are clearly visible in the region of mesopores filling, and show H3 characteristics, which can be attributed to slit-shaped pores. It is worth noting that the isotherms of SMCT-12 show an unconspicuous hysteresis loop, indicating a low BET surface area and mesoporosity. Furthermore, the area of hysteresis loop of SMCT-24 is little bigger than that of SMCT-48, probably revealing the bigger nitrogen adsorption capacity of SMCT-24 in mesoporous range.

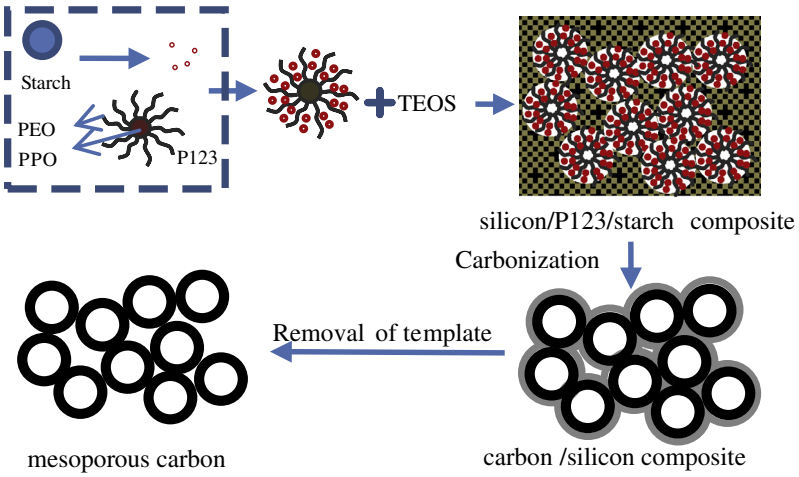

Fig. 1. Synthesis schematic of SMC.

The pore structural parameters of SMCs are given in Table 1. The results indicate that S_{BET}, V_t and mesoporosity go through maximum as the crystallization time increases from 12 to 48 h. Appropriate crystallization time, i.e. 24 h in this experiment, can greatly improve S_{BET} and mesoporosity of SMC. For all of the as-made SMCs, their mesoporosity is in the range of 68.6–95.0%, further evidencing that the as-made SMCs are mainly composed of mesopores. For SMCT-24, its average pore size is about 3.5 nm, which can be clearly seen from the inset in Fig. 2. S_{BET} of SMCT-24 is as high as 1157 $m^2 g^{-1}$, its total pore volume and mesoporosity are 0.97 $cm^3 g^{-1}$ and up to 95.0%, respectively. During the crystallization process, P123, starch and silicon can co-assemble, and the crystallization time plays an important role on the assembly degree. When the crystallization time is short (e.g. 12 h), the degree of the assembly is low so that some porous structures have no enough time to form, resulting in the low BET surface area of SMC. However, due to the excessive assembly under long crystallization time (e.g. 48 h), some previous formed pores are blocked, causing the decrease in the BET surface area of SMCs. This indicates that appropriate crystallization time can greatly improve the mesoporosity as well as the mesoporous structure.

TEM measurement also can be used to reveal the pore structure of SMCs as shown in Fig. 3. TEM images in Fig. 3(a–c) are seen from [1 1 0] direction while TEM image in Fig. 3(d) is viewed from [1 0 0] direction. From the TEM image of SMCT-12 shown in Fig. 3(a), SMCT-12 is found having an irregular morphology. Compared with SMCT-12, TEM images of SMCT-24 in Fig. 3(b) and SMCT-48 in Fig. 3(c) have ordered mesostructure and uniform pore size distribution. It is noted that the pore diameter of SMCT-48 is little smaller than that of SMCT-24, which is consistent with the pore diameter calculated from N_2 adsorption/desorption isotherms as listed in Table 1. These results demonstrate that P123 and TEOS have been homogeneously mixed with starch, thus forming uniform mesopores.

Fig. 4(a) gives the FTIR spectra of SMCs. The peak at 1629 cm^{-1} is the characteristic of —C=C stretching vibration, and the band at 2900 cm^{-1} is due to the —C—H stretching vibration [26]. The big peak at 3440 cm^{-1} is due to the —O—H stretching vibration, ensuring the hydrophilicity and wettability of SMCs, which are beneficial for SMCs to be used as electrode material in the aqueous supercapacitor [27].

As can be observed in Fig. 4(b), the Raman spectra of the SMCs feature two major peaks centered at 1350 cm^{-1} (D-band) and 1580 cm^{-1} (G-band) for carbon materials, which are ascribed to the defects/imperfections and hexagonal graphene plane, respectively. The relative intensity ratio of the D and G bands (I_D/I_G) not only depends on the type of graphitic materials, but also correlates with the degree of crystallinity. The intensity ratio of I_D/I_G changes from 1.87 to 1.59 and 1.88 with increasing crystallization time, indicating that SMCT-24 appears to have a better crystallinity than SMCT-12 and SMCT-48.

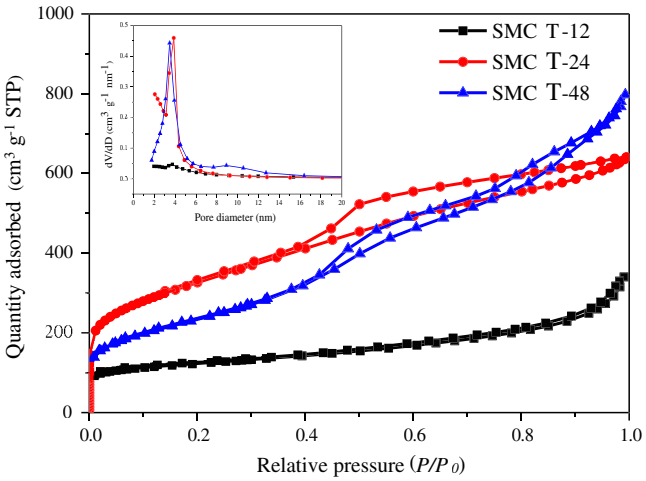

Fig. 2. N_2 adsorption–desorption isotherms of SMCs.

3.3. Electrochemical properties

Galvanostatic charge–discharge cycling has been employed to evaluate the capacitance of SMC electrodes. Fig. 5(a) shows the typical charge–discharge profile of SMC electrodes in 6 M KOH electrolyte at room temperature. The shapes of the charge curves are closely linear in the potential range studied and the discharge curves are almost symmetric with their corresponding charge

Table 1
Pore structural parameters of SMCs.

Samples	S_{BET} ($m^2 g^{-1}$)	V_t ($cm^3 g^{-1}$)	Mesoporosity (%)	Mean pore diameter (nm)
SMCT-12	441	0.49	72.7	3.7
SMCT-24	1157	0.97	95.0	3.5
SMCT-48	841	1.19	68.6	3.4

S_{BET}: BET surface area, $m^2 g^{-1}$; V_t: total volume volume, $cm^3 g^{-1}$; mesoporosity: the ratio of mesopore volume to total pore volume, %.

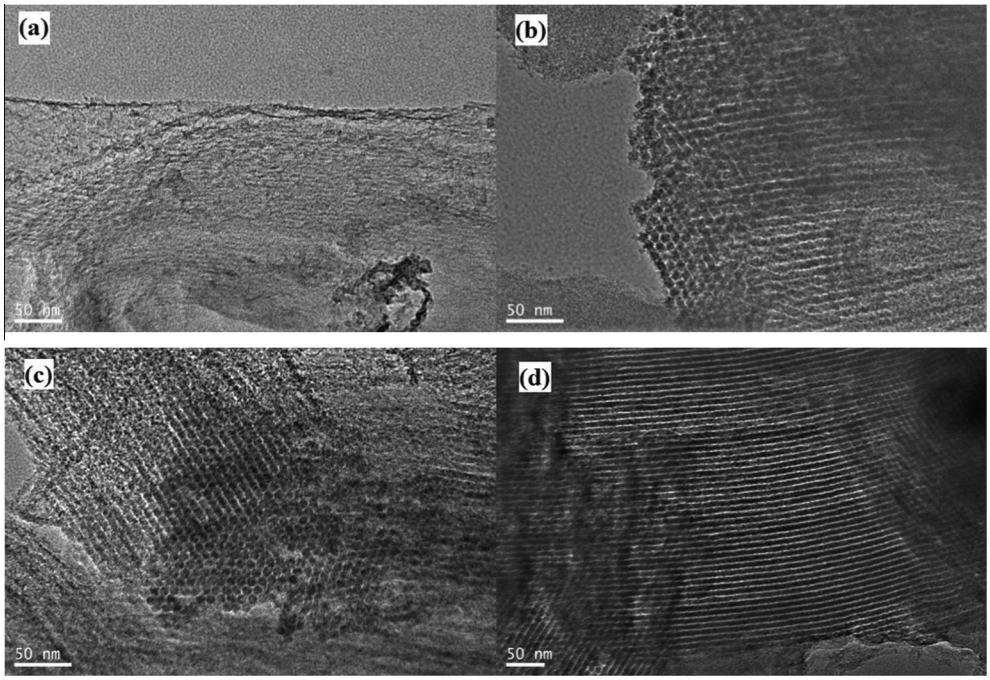

Fig. 3. TEM images of SMCT-12 (a), SMCT-24 (b and d) and SMCT-48 (c).

curves, all of which indicate the good capacitive properties of SMC electrodes [28].

Furthermore, galvanostatic discharge test is known as the most accurate method for capacitance evaluation [29]. Fig. 5(b) is the discharge curves of SMCT-24 electrode at different current densities. The discharge time of SMCT-24 electrode can remarkably shorten with increasing current density, indicating that the electrolyte ions have sufficient time to enter and diffuse into the pores of SMC electrodes in the wide current density of 50–400 mA g^{-1}.

The specific capacitance (C, F g^{-1}) of SMC electrode based on the mass of active materials can be calculated from the slope of the discharge curve according to Eq. (1) [30,31].

$$C = 2I \cdot \Delta t/(\Delta V \cdot m) \quad (1)$$

where I (A) is the discharge current, $\triangle V$ (V) is the discharge voltage difference between the $\triangle t$ (s) period, and m (g) is the mass of the active material in one electrode.

The charge/discharge performance at high current density is often chosen to estimate the capacitive properties. The higher the capacitance retention at high current density means the better capacitive performance of electrode. Fig. 6 gives the specific capacitance of SMC electrodes vs. current density, from which it can be seen that the specific capacitance of SMC electrodes decrease slowly with increasing current density. The decrease of the specific capacitance results mainly from high polarization of electrode and ohmic drop at high current density, which can be explained by the decreasing accessibility of ions into the active layer in the electrode matrices with increasing current density [32]. The highest specific capacitance at the current density of 50 mA g^{-1} is 144 F g^{-1} for SMCT-24 electrode, compared with 80 F g^{-1} for SMCT-12 electrode and 89 F g^{-1} for SMCT-48 electrode. As mentioned above, the mesoporosity and S_{BET} of SMCT-24 are the highest among the three SMCs samples. It is deduced that the solvated ions can fast diffuse into the pores of SMCT-24 electrode even at high current load. Therefore, high mesoporosity plays important roles in the rate capability. The SMCT-24 electrode can possess high capacitance retention as ca. 72.4% at the current density of 1000 mA g^{-1}, clearly revealing the fast diffuse of solvated ions into the mesopores of SMCT-24 even at high current desnity, and its high rate capacity. It is believed that both larger mesopore size and high mesopore fraction mainly determine the high rate capability of SMC electrodes. These results indicate that SMC with high mesoporosity is a very promising electrode material in electrochemical area.

Durability also is one of the most important features for the practical application of capacitor [33–35]. Fig. 7 presents the specific capacitance of SMCT-24 vs. cycle number at 50 mA g^{-1} of the current density. After 1000 cycles, the specific capacitance has a gradual decrease and the capacitance retention is as high as 88.5%, which is still much higher than reported MC materials [36–38]. The SMCT-24 electrode maintains its capacity fairly well over time, indicating its high electrochemical reproducibility as well as good interfacial contact after long-term charge/discharge. The slight capacitance drop may be related to some irreversible reactions caused by the functional groups in SMCT-24 (see Fig. 4).

Fig. 8 presents the CV curves of SMC electrodes at 2–10 mV s^{-1} of scan rates in 6 M KOH aqueous electrolyte. For an ideal EDLC, the kinetic process of ion transfer is not limited. It will be a rectangular-shaped curve of current versus potential if the responding current keeps a constant at a certain scan rate in the CV measurements. The rectangular degree of the CV curves reflects the ion diffusion rate within the pores of electrodes. The higher the rectangular degree is, the bigger the ion diffusion rate will be. As shown in Fig. 8(a and b), the SMC electrodes exhibit good rectangular shapes, showing almost mirror images with respect to the zero-current line, which are characteristic of EDLC [39,40]. The rectangular-shaped CV curves gradually collapse with increasing scan rate as shown in Fig. 8(b), which may be caused by the significant contribution of the equivalent series resistance associated with the capacitor. This behavior has also been observed in other MC electrode [41].

As a powerful technique for the investigation of the capacitive behavior of capacitor, electrochemical impedance spectroscopy (EIS) has also been used to check the ability of MC to store electrical energy [42,43]. Nyquist plots of SMC electrodes, also known as EIS, are presented in Fig. 9. All plots exhibit two distinct traits: a semicircle in the high frequency range and a sloped line in the

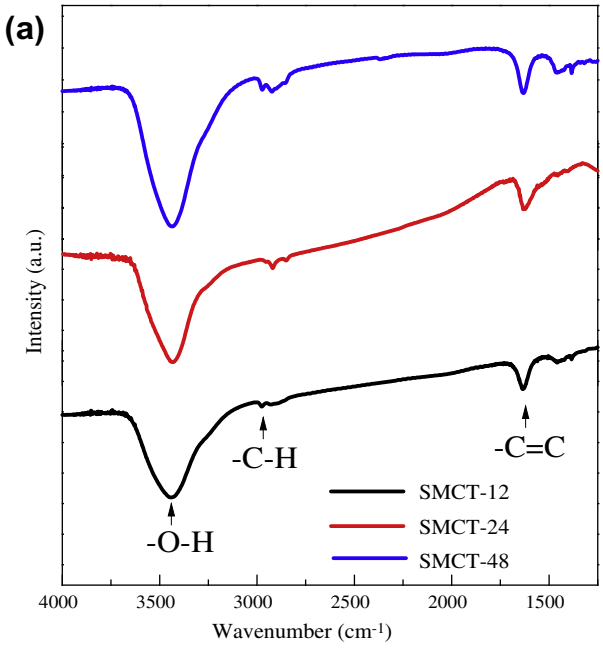

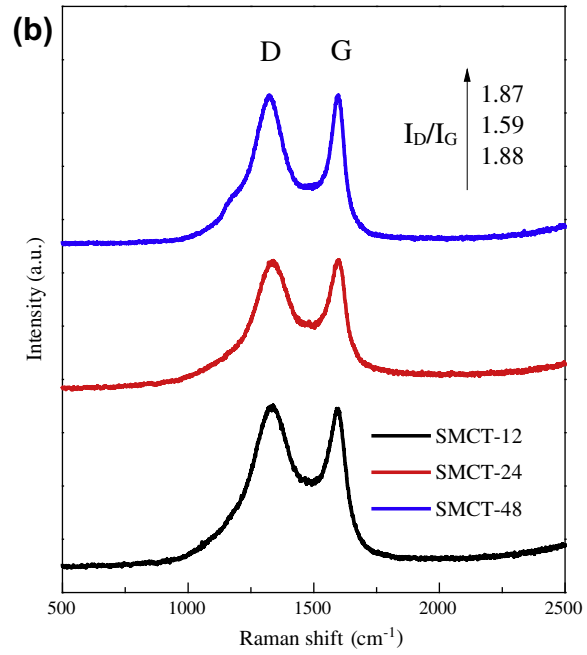

Fig. 4. FTIR spectra of SMCs (a) and Raman spectra of SMCs (b).

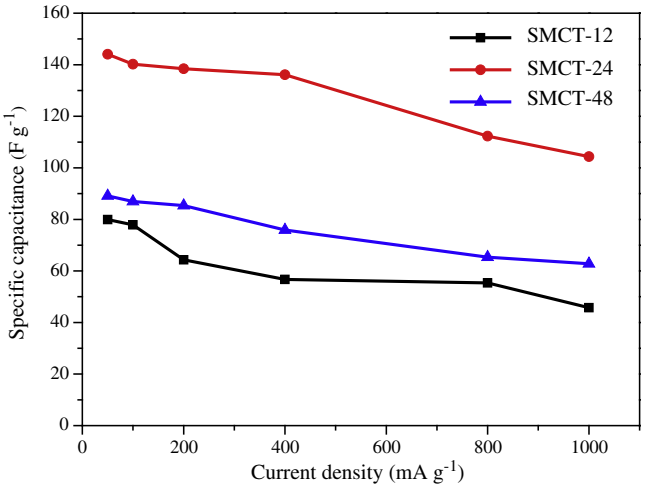

Fig. 6. Specific capacitance of SMC electrodes vs. current density.

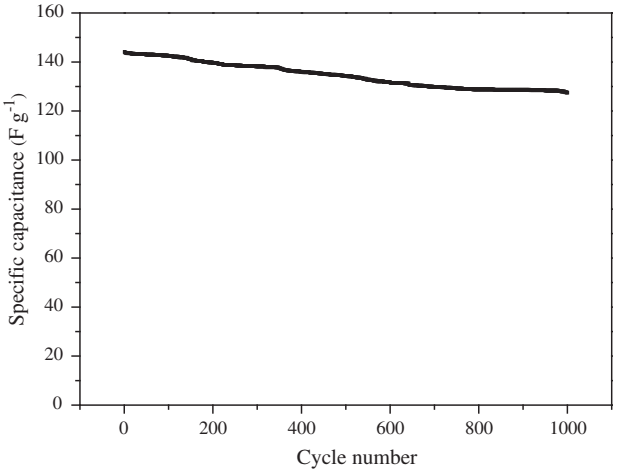

Fig. 7. Effect of cycle number on the specific capacitance of SMCT-24 electrode.

low frequency range. The semicircle in the high frequency region is correlated with the resistance of the SMC electrode itself and the contact resistance between SMC electrode and current collector. At low frequency, the imaginary part sharply increases and a nearly vertical line is observed, suggesting the pure capacitive behavior of the SMC electrode.

The charge–discharge performance can be reflected by the value of knee frequency. The higher value of the knee frequency is,

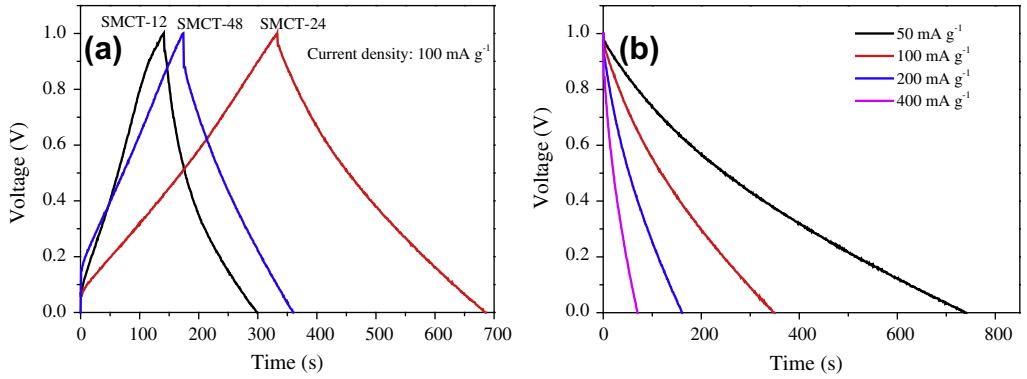

Fig. 5. (a) Charge–discharge curves of SMC electrodes at the current density of 100 mA g^{-1}, and (b) discharge curves of SMCT-24 electrode at different current densities.

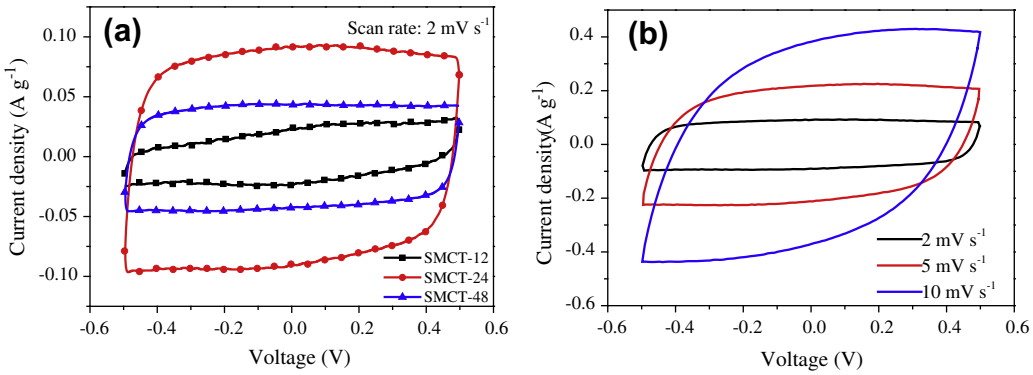

Fig. 8. (a) Cyclic voltammetry curves of SMC electrodes at the scan rate of 2 mV s^{-1}, and (b) cyclic voltammetry curves of SMCT-24 electrode at different scan rates.

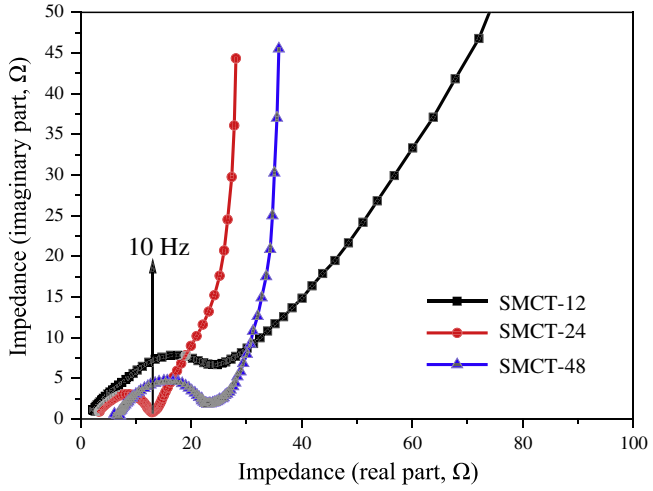

Fig. 9. Nyquist plots of the SMC electrodes.

the easier the accessibility of hydrated ions into the pores and the better performance of fast charge and discharge. It is worth noting that the knee frequency of the SMCT-24 electrode is 10 Hz, which is much higher than most reported MCs [42,44]. This illustrates that the capacitor with SMC electrode can charge/discharge more rapidly, in other words, it has a high power density [45].

4. Conclusion

High performance SMC for EDLC was prepared by a simultaneous template method. It has been found that the specific capacitance of SMCT-24 electrode at the current density of 50 mA g^{-1} was 144 F g^{-1}, and remained at 127 F g^{-1} even after 1000 cycles. The results demonstrated that the synthesis method described in this work was of potential to make SMC with high performance for EDLC. SMC mainly composed of mesopores is a sort of competitive electrode materials for EDLC, both in terms of capacitance retention and rate capability.

Acknowledgements

This work was supported by the National Natural Science Foundation of China (Nos. 20876176, 51172285, 51272004, 51372277); the Fundamental Research Funds for the Central Universities (CX-1217, 14CX06045A, 14CX02060A, 13CX05011A).

References

[1] R. Kötz, M. Carlen, Principles and applications of electrochemical capacitors, Electrochim. Acta 45 (2000) 2483–2498.
[2] M. Endo, Y.J. Kim, H. Ohta, K. Ishii, T. Inoue, T. Hayashi, Y. Nishimura, T. Maeda, M.S. Dresselhaus, Morphology and organic EDLC applications of chemically activated AR-resin-based carbons, Carbon 40 (2002) 2613–2626.
[3] D.W. Wang, F. Li, M. Liu, G.Q. Lu, H.-M. Cheng, 3D aperiodic hierarchical porous graphitic carbon material for high-rate electrochemical capacitive energy storage, Angew. Chem. 120 (2008) 379–382.
[4] G. Lota, E. Frackowiak, Striking capacitance of carbon/iodide interface, Electrochem. Commun. 11 (2009) 87–90.
[5] C.C. Wang, C.C. Hu, Electrochemical catalytic modification of activated carbon fabrics by ruthenium chloride for supercapacitors, Carbon 43 (2005) 1926–1935.
[6] K.W. Nam, C.W. Lee, X.Q. Yang, B.W. Cho, W.S. Yoon, K.B. Kim, Electrodeposited manganese oxides on three-dimensional carbon nanotube substrate: supercapacitive behaviour in aqueous and organic electrolytes, J. Power Sources 188 (2009) 323–331.
[7] H. Shi, Activated carbons and double layer capacitance, Electrochim. Acta 41 (1996) 1633–1639.
[8] D. Qu, H. Shi, Studies of activated carbons used in double-layer capacitors, J. Power Sources 74 (1998) 99–107.
[9] X. Shao, W. Wang, R. Xue, Z. Shen, Adsorption of methane and hydrogen on mesocarbon microbeads by experiment and molecular simulation, J. Phys. Chem. B 108 (2004) 2970–2978.
[10] E. Frackowiak, K. Jurewicz, K. Szostak, S. Delpeux, F. Béguin, Nanotubular materials as electrodes for supercapacitors, Fuel Process. Technol. 77–78 (2002) 213–219.
[11] K. Kierzek, E. Frackowiak, G. Lota, G. Gryglewicz, J. Machnikowski, Electrochemical capacitors based on highly porous carbons prepared by KOH activation, Electrochim. Acta 49 (2004) 515–523.
[12] L. Ding, B. Zou, H. Liu, Y. Li, Z. Wang, Y. Su, Y. Guo, X. Wang, A new route for conversion of corncob to porous carbon by hydrolysis and activation, Chem. Eng. J. 225 (2013) 300–305.
[13] A.G. Pandolfo, A.F. Hollenkamp, Carbon properties and their role in supercapacitors, J. Power Sources 157 (2006) 11–27.
[14] S. Mitani, S.-I. Lee, S.-H. Yoon, Y. Korai, I. Mochida, Activation of raw pitch coke with alkali hydroxide to prepare high performance carbon for electric double layer capacitor, J. Power Sources 133 (2004) 298–301.
[15] B. Xu, F. Wu, R. Chen, G. Cao, S. Chen, Z. Zhou, Y. Yang, Highly mesoporous and high surface area carbon: a high capacitance electrode material for EDLCs with various electrolytes, Electrochem. Commun. 10 (2008) 795–797.
[16] R.W. Pekala, Organic aerogels from the polycondensation of resorcinol with formaldehyde, J. Mater. Sci. 24 (1989) 3221–3227.
[17] S.A. Al-Muhtaseb, J.A. Ritter, Preparation and properties of resorcinol–formaldehyde organic and carbon gels, Adv. Mater. 15 (2003) 101–114.
[18] T. Kyotani, Control of pore structure in carbon, Carbon 38 (2000) 269–286.
[19] J.H. Knox, B. Kaur, G.R. Millward, Structure and performance of porous graphitic carbon in liquid chromatography, J. Chromatogr. A 352 (1986) 3–25.
[20] D. Kawashima, T. Aihara, Y. Kobayashi, T. Kyotani, A. Tomita, Preparation of mesoporous carbon from organic polymer/silica nanocomposite, Chem. Mater. 12 (2000) 3397–3401.
[21] W. Sui, J. Zheng, Z. Yang, M. Wu, A simple method of preparing ordered and three-dimensionally-interconnected macroporous carbon with mesoporosity by using silica template, Mater. Lett. 65 (2011) 2534–2536.
[22] Z.H. Hou, X.H. Li, Z.Q. He, E.H. Liu, L.F. Deng, New mesoporous carbon prepared by a simultaneous synthetic template carbonization method, J. Mater. Sci. 39 (2004) 3793–3795.
[23] M.Z. Momčilović, M.S. Ranđelović, A.R. Zarubica, A.E. Onjia, M. Kokunešoski, B.Z. Matović, SBA-15 templated mesoporous carbons for 2,4-dichlorophenoxyacetic acid removal, Chem. Eng. J. 220 (2013) 276–283.

[24] D.Y. Zhao, J.L. Feng, Q.S. Huo, N. Melosh, G.H. Fredrickson, B.F. Chmelka, G.D. Stucky, Triblock copolymer syntheses of mesoporous silica with periodic 50–300 angstrom pores, Science 279 (1998) 548–552.
[25] K. Schillén, J. Jansson, D. Löf, T. Costa, Mixed micelles of a PEO–PPO–PEO triblock compolymer (P123) and a nonionic surfactant (C12EO6) in water. A dynamic and static light scattering study, J. Phys. Chem. B 112 (2008) 5551–5562.
[26] D.J. Kim, H.I. Lee, J.E. Yie, S.J. Kim, J.M. Kim, Ordered mesoporous carbons: implication of surface chemistry, pore structure and adsorption of methyl mercaptan, Carbon 43 (2005) 1868–1873.
[27] D.S. Yuan, J.H. Zeng, J.X. Chen, Y.L. Liu, Highly ordered mesoporous carbon synthesized via in situ template for supercapacitors, Int. J. Electrochem. Sci. 4 (2009) 562–570.
[28] Q. Huang, X. Wang, J. Li, C. Dai, S. Gamboa, P.J. Sebastian, Nickel hydroxide/activated carbon composite electrodes for electrochemical capacitors, J. Power Sources 164 (2007) 425–429.
[29] Q. Cheng, J. Tang, J. Ma, H. Zhang, N. Shinya, L.C. Qin, Graphene and carbon nanotube composite electrodes for supercapacitors with ultra-high energy density, Phys. Chem. Chem. Phys. 13 (2011) 17615–17624.
[30] X. Li, W. Xing, S. Zhuo, J. Zhou, F. Li, S.Z. Qiao, G.Q. Lu, Preparation of capacitor's electrode from sunflower seed shell, Bioresour. Technol. 102 (2011) 1118–1123.
[31] C. Portet, G. Yushin, Y. Gogotsi, Effect of carbon particle size on electrochemical performance of EDLC, J. Electrochem. Soc. 155 (2008) A531–A536.
[32] C. Kim, S.H. Park, W.J. Lee, K.S. Yang, Characteristics of supercapaitor electrodes of PBI-based carbon nanofiber web prepared by electrospinning, Electrochim. Acta 50 (2004) 877–881.
[33] W.G. Pell, B.E. Conway, N. Marincic, Analysis of non-uniform charge/discharge and rate effects in porous carbon capacitors containing sub-optimal electrolyte concentrations, J. Electroanal. Chem. 491 (2000) 9–21.
[34] J. Chmiola, G. Yushin, R. Dash, Y. Gogotsi, Effect of pore size and surface area of carbide derived carbons on specific capacitance, J. Power Sources 158 (2006) 765–772.
[35] X. He, P. Ling, M. Yu, X. Wang, X. Zhang, M. Zheng, Rice husk-derived porous carbons with high capacitance by $ZnCl_2$ activation for supercapacitors, Electrochim. Acta 105 (2013) 635–641.
[36] Y.Q. Dou, Y. Zhai, H. Liu, Y. Xia, B. Tu, D. Zhao, X.X. Liu, Syntheses of polyaniline/ordered mesoporous carbon composites with interpenetrating framework and their electrochemical capacitive performance in alkaline solution, J. Power Sources 196 (2011) 1608–1614.
[37] A.B. Fuertes, F. Pico, J.M. Rojo, Influence of pore structure on electric double-layer capacitance of template mesoporous carbons, J. Power Sources 133 (2004) 329–336.
[38] J. Wang, C. Xue, Y. Lv, F. Zhang, B. Tu, D. Zhao, Kilogram-scale synthesis of ordered mesoporous carbons and their electrochemical performance, Carbon 49 (2011) 4580–4588.
[39] C. Du, N. Pan, High power density supercapacitor electrodes of carbon nanotube films by electrophoretic deposition, Nanotechnology 17 (2006) 5314.
[40] X. He, R. Li, J. Qiu, K. Xie, P. Ling, M. Yu, X. Zhang, M. Zheng, Synthesis of mesoporous carbons for supercapacitors from coal tar pitch by coupling microwave-assisted KOH activation with a MgO template, Carbon 50 (2012) 4911–4921.
[41] S. Yoon, J. Lee, T. Hyeon, S.M. Oh, Electric double-layer capacitor performance of a new mesoporous carbon, J. Electrochem. Soc. 147 (2000) 2507–2512.
[42] E. Frackowiak, F. Béguin, Carbon materials for the electrochemical storage of energy in capacitors, Carbon 39 (2001) 937–950.
[43] W. Wei, X. Cui, W. Chen, D.G. Ivey, Improved electrochemical impedance response induced by morphological and structural evolution in nanocrystalline MnO_2 electrodes, Electrochim. Acta 54 (2009) 2271–2275.
[44] Q.Y. Li, H.Q. Wang, Q.F. Dai, J.H. Yang, Y.L. Zhong, Novel activated carbons as electrode materials for electrochemical capacitors from a series of starch, Solid State Ionics 179 (2008) 269–273.
[45] G.A. Snook, C. Peng, D.J. Fray, G.Z. Chen, Achieving high electrode specific capacitance with materials of low mass specific capacitance: potentiostatically grown thick micro-nanoporous PEDOT films, Electrochem. Commun. 9 (2007) 83–88.